Toxicology in Vitro 24 (2010) 1554–1561

Contents lists available at ScienceDirect

Toxicology in Vitro

journal homepage: www.elsevier.com/locate/toxinvit

Modulation of NAD(P)H:quinone oxidoreductase by vanadium in human hepatoma HepG2 cells

Ghada Abdelhamid [a,b], Anwar Anwar-Mohamed [a], Mohey M. Elmazar [c], Ayman O.S. El-Kadi [a,*]

[a] Faculty of Pharmacy and Pharmaceutical Sciences, University of Alberta, Edmonton, Alberta, Canada T6G 2N8
[b] Department of Pharmacology and Toxicology, Faculty of Pharmacy, Helwan University, Helwan, Egypt
[c] Department of Pharmacology and Toxicology, Faculty of Pharmacy, Ahram Canadian University, 6 of October, Egypt

ARTICLE INFO

Article history:
Received 6 April 2010
Accepted 23 June 2010
Available online 3 July 2010

Keywords:
Aryl hydrocarbon receptor
NQO1
Vanadium
Carcinogenesis

ABSTRACT

Recent studies demonstrated the carcinogenicity and the mutagenicity of vanadium compounds. In addition, vanadium (V^{5+}) was found to enhance the effects of other genotoxic agents. However, the mechanism by which V^{5+} induce toxicity remain unknown. In the current study we examined the effect of V^{5+} (as ammonium metavanadate, NH_4VO_3) on the expression of NAD(P)H: quinone oxidoreductase 1 (NQO1) in human hepatoma HepG2 cells. Therefore, HepG2 cells were treated with increasing concentrations of V^{5+} in the presence of two NQO1 inducers, the 2,3,7,8-tetrachlorodibenzo-*p*-dioxin (TCDD) and isothiocyanate sulforaphane (SUL). Our results showed that V^{5+} inhibited the TCDD- and SUL-mediated induction of NQO1 at mRNA, protein and activity levels. Investigating the effect of V^{5+} at transcriptional levels revealed that V^{5+} significantly inhibited the TCDD- and SUL-mediated induction of antioxidant responsive element (ARE)-dependent luciferase reporter gene expression. In addition, V^{5+} was able to decrease the TCDD- and SUL-induced nuclear accumulation of nuclear factor erythroid 2-related factor-2 (Nrf2) without affecting Nrf2 mRNA or protein levels. Looking at the post-transcriptional level, V^{5+} did not affect NQO1 mRNA stability, thus eliminating the possible role of V^{5+} in decreasing NQO1 mRNA levels through this mechanism. In contrast, at post-translational level, V^{5+} was able to significantly decrease NQO1 protein half-life. The present study demonstrates for the first time that V^{5+} down-regulates NQO1 at the transcriptional and post-translational levels in the human hepatoma HepG2 cells via AhR- and Nrf2-dependent mechanisms.

1. Introduction

NAD(P)H:quinone oxidoreductase 1 (NQO1) is a phase II metabolizing enzyme that has been shown to play an essential role in the detoxification of xenobiotics and carcinogenic metabolites (Chen and Kunsch, 2004; Lee and Johnson, 2004; Rushmore and Kong, 2002; Xu et al., 2005). Several studies have demonstrated a complex regulation of NQO1, in which the transcriptional activation of this gene is regulated by both xenobiotic responsive element (XRE) and antioxidant responsive element (ARE) (Chen and Kunsch, 2004; Miao et al., 2005; Nioi and Hayes, 2004). The mechanisms governing the induction of this gene are of important, because NQO1 enzymatic activity is used as an index of chemoprotective efficacy for anti-carcinogenic agents (Prochaska and Santamaria, 1988).

NQO1 gene expression can be induced through two separate regulatory elements associated with its 5′-flanking region. The first pathway includes activation of a cytosolic transcription factor, the aryl hydrocarbon receptor (AhR) (Anwar-Mohamed and El-Kadi, 2009). The inactive form of AhR is attached to a complex of two heat shock proteins 90 (HSP90), hepatitis B virus X-associated protein (XAP2), and the chaperone protein p23 (Hankinson, 1995; Meyer et al., 1998). Upon ligand binding, the AhR-ligand complex dissociates from the cytoplasmic complex and translocates to the nucleus where it associates with the aryl hydrocarbon nuclear translocator (Arnt) (Whitelaw et al., 1994). The whole complex then acts as a transcription factor to mediate the induction of NQO1 through activating the XRE located in its promoter region (Prochaska and Talalay, 1988). The second pathway involves activation of the ARE. In fact, the increased expression of NQO1 gene expression in response to oxidative stress caused by agents such as isothiocyanate sulforaphane (SUL), tert-butylhydroquinone (t-BHQ) and H_2O_2 occurs through this signaling pathway (Itoh et al., 1997). The redox status of the cell activates the nuclear factor erythroid 2-related factor-2 (Nrf2), a redox-sensitive member of the cap 'n' collar basic leucine zipper (CNC bZip) family of

* Corresponding author. Address: Faculty of Pharmacy and Pharmaceutical Sciences, 3126 Dentistry/Pharmacy Centre, University of Alberta, Edmonton, Alberta, Canada T6G 2N8. Tel.: +1 780 492 3071; fax: +1 780 492 1217.
E-mail address: aelkadi@pharmacy.ualberta.ca (A.O.S. El-Kadi).

0887-2333/$ - see front matter © 2010 Elsevier Ltd. All rights reserved.
doi:10.1016/j.tiv.2010.06.017

transcription factors (Itoh et al., 1997). Subsequently, Nrf2 dissociates from its cytoplasmic tethering polypeptide, Kelch-like ECH associating protein 1 (Keap1), and then translocates into the nucleus, dimerizes with a musculoaponeurotic fibrosarcoma (MAF) protein, thereafter binds to and activate ARE (Ma et al., 2004). The Nrf2/ARE signaling pathway plays an important role in cellular protection in response to oxidative stresses (Motohashi and Yamamoto, 2004). For example, Nrf2-deficient mice are more susceptible than wild-type mice to oxidative injury and chemical-induced carcinogenesis (Iida et al., 2004). Therefore, the Nrf2/ARE signaling pathway is a main target to study novel chemopreventive agents (Ai et al., 2009; Lee and Surh, 2005; Yu and Kensler, 2005).

Many studies have examined the toxic effects of individual AhR ligands, yet there have been very few studies on the combined toxic effects of AhR ligands and other environmental co-contaminants. Among these, environmental co-contaminants of most concern are heavy metals, typified by vanadium (V^{5+}). Environmental contamination by V^{5+} has dramatically increased during the last decades, especially in the most developed countries, due to the widespread use of fossil fuels, many of which liberate fine particulates of V^{5+} to the atmosphere during combustion (Baran, 2008). Humans consume appreciable amounts of V^{5+} in food and water (Evangelou, 2002). The estimated daily intake of V^{5+} is 10–60 μg (Nechay, 1984). Furthermore, weight training athletes are reported to use up to 18.6 mg V^{5+} per day as a body-building supplement (Barceloux, 1999). An estimate of the total body pool of vanadium in healthy individuals is 100–200 μg (Haiman et al., 2003). If we take into consideration the fact that heavy metals such as V^{5+} are significantly deposited in hepatocytes and kidneys (Edel and Sabbioni, 1989), the concentrations used in the current study are of great relevance to those in humans.

Recently, we have demonstrated that V^{5+} down-regulates the bioactivating enzyme CYP1A1 which is solely under the control of XRE, through a transcriptional mechanism (Abdelhamid et al., 2010). Therefore, the current study aims to address the possible effect of this metal on the NQO1 gene expression in human hepatoma HepG2 cells.

2. Materials and methods

2.1. Materials

Ammonium metavanadate (NH_4VO_3), cycloheximide (CHX), 2,6-dichlorophenolindophenol, dicoumarol, isothiocyanate sulforaphane and protease inhibitor cocktail were purchased from Sigma–Aldrich (St. Louis, MO). 2,3,7,8-Tetrachlorodibenzo-*p*-dioxin, >99% pure, was purchased from Cambridge Isotope Laboratories (Woburn, MA). TRIzol reagent and Lipofectamine 2000 reagents were purchased from Invitrogen (San Diego, CA). The High-Capacity cDNA reverse transcription kit and SYBR Green PCR master mix were purchased from Applied Biosystems (Foster City, CA). Actinomycin-D (Act-D) was purchased from Calbiochem (San Diego, CA). Chemiluminescence Western blotting detection reagents were from GE Healthcare Life Sciences (Piscataway, NJ). Nitrocellulose membrane was purchased from Bio-Rad (Hercules, CA). NAD(P)H:quinone oxidoreductase 1 (NQO1) rabbit polyclonal primary antibody (ab34173) was purchased from abcam, Inc. (Abcam-Cambridge, Massachusetts (MA), USA), anti-rabbit IgG peroxidase secondary antibody was purchased from Santa Cruz Biotechnology, Inc. (Santa Cruz, CA), nuclear factor erythroid 2-related factor-2 (Nrf2) mouse monoclonal primary antibody (MAB3925), anti-mouse IgG peroxidase secondary antibody were purchased from R&D Systems, (Minneapolis, MN, USA). pRL-CMV plasmid and dual luciferase assay reagents were obtained from Promega (Madison, WI). All other chemicals were purchased from Thermo Fisher Scientific (Toronto, ON, Canada). Primers were purchased from Integrated DNA Technologies, Inc. (Coralville, IA) and are listed in Table 1.

2.2. Cell culture

Human hepatoma HepG2 cell line, ATCC number HB-8065 (Manassas, VA), was maintained in Dulbecco's modified Eagle's medium (DMEM) supplemented with 10% heat-inactivated fetal bovine serum, and 1% penicillin–streptomycin. Cells were grown in 75-cm^2 cell culture flasks at 37 °C in a 5% CO_2 humidified incubator.

2.3. Chemical treatments

Cells were treated in serum-free medium with various concentrations of V^{5+} (25–250 μM) in the absence and presence of 1 nM TCDD or 5 μM SUL as described in figure legends. TCDD and SUL were dissolved in dimethyl sulfoxide (DMSO) and maintained in DMSO at −20 °C until use. V^{5+} was prepared freshly in double deionized water. In all treatments, the DMSO concentration did not exceed 0.05% (v/v).

2.4. RNA extraction and cDNA synthesis

Six hours after incubation with the test compounds, cells were collected and total RNA was isolated using TRIzol reagent (Invitrogen) according to the manufacturer's instructions, and quantified by measuring the absorbance at 260 nm. Thereafter, first-strand cDNA synthesis was performed by using the High-Capacity cDNA reverse transcription kit (Applied Biosystems) according to the manufacturer's instructions. Briefly, 1.5 μg of total RNA from each sample was added to a mix of 2.0 μl 10X RT buffer, 0.8 μl 25X dNTP mix (100 mM), 2.0 μl 10X RT random primers, 1.0 μl MultiScribe™ reverse transcriptase and 3.2 μl nuclease-free water. The final reaction mix was kept at 25 °C for 10 min, heated to 37 °C for 120 min, heated for 85 °C for 5 s and finally cooled to 4 °C.

2.5. Quantification by real time-PCR

Quantitative analysis of specific mRNA expression was performed by real time-PCR, by subjecting the resulting cDNA to PCR amplification using 96-well optical reaction plates in the ABI Prism 7500 System (Applied Biosystems). About 25-μl reaction mix contained 0.1 μl of 10 μM forward primer and 0.1 μl of 10 μM reverse primer (40 nM final concentration of each primer), 12.5 μl of SYBR Green Universal Mastermix, 11.05 μl of nuclease-free water and 1.25 μl of cDNA sample. The primers used in the current study were chosen from previously published studies (Rushworth et al., 2008; Westerink and Schoonen, 2007) and are listed in Table 1. Thermocycling conditions were initiated at 95 °C for 10 min, followed by 40 PCR cycles of denaturation at 95 °C for 15 s and anneal/extension at 60 °C for 1 min.

Table 1
Primers sequences used for real-time PCR reactions.

Gene	Forward primer	Reverse primer
NQO1	5′-CGC AGA CCT TGT GAT ATT CCA G-3′	5′-CGT TTC TTC CAT CCT TCC AGG-3′
Nrf2	5′-AAC CAC CCT GAA AGC ACA GC-3′	5′-TGA AAT GCC GGA GTC AGA ATC-3′
β-Actin	5′-CTG GCA CCC AGC ACA ATG-3′	5′-GCC GAT CCA CAC GGA GTA CT-3′

2.6. Real time-PCR data analysis

The real time-PCR data were analyzed using the relative gene expression i.e. ($\Delta\Delta C_T$) method as described in Applied Biosystems User Bulletin No. 2 and explained further by Livak and Schmittgen (2001). Briefly, the ΔC_T values were calculated in every sample for each gene of interest as follows: $C_{T\text{gene of interest}} - C_{T\text{reporter gene}}$, with β-actin as the reporter gene. Calculation of relative changes in the expression level of one specific gene ($\Delta\Delta C_T$) was performed by subtraction of ΔC_T of control (untreated cells or 0 h time point) from the ΔC_T of the corresponding treatment groups. The values and ranges given in different figures were determined as follows: $2^{-\Delta(\Delta C_T)}$ with $\Delta\Delta C_T$ + S.E. and $\Delta\Delta C_T$ − S.E., where S.E. is the standard error of the mean of the $\Delta(\Delta C_T)$ value.

2.7. Protein extraction and Western blot analysis

Twenty-four hours after incubation with the test compounds, cells were collected in lysis buffer as described previously (Anwar-Mohamed and El-Kadi, 2009). Proteins for NQO1 (5 μg), or Nrf2 (25 μg) were resolved by denaturing electrophoresis, as described previously (Sambrook et al., 1989). Briefly, the cell homogenates were dissolved in 1X sample buffer, boiled for 5 min, separated by 10% SDS–PAGE and electrophoretically transferred to a nitrocellulose membrane. Protein blots were blocked for 24 h at 4 °C in blocking buffer containing 5% skim milk powder, 2% bovine serum albumin and 0.05% (v/v) Tween 20 in Tris-buffered saline solution (0.15 M sodium chloride, 3 mM potassium chloride and 25 mM Tris base). After blocking, the blots were incubated with NQO1 rabbit polyclonal primary antibody for 2 h at room temperature or Nrf2 mouse monoclonal primary antibody for 24 h at 4 °C in Tris-buffered saline containing 0.05% (v/v) Tween 20 and 0.02% sodium azide. Incubation with a peroxidase-conjugated goat anti-rabbit IgG secondary antibody for NQO1 or anti-mouse IgG secondary antibody for Nrf2 was carried out in blocking buffer for 1 h at room temperature. The bands were visualized with the enhanced chemiluminescence method according to the manufacturer's instructions (GE Healthcare, Piscataway, NJ). The intensity of protein bands was quantified relative to the signals obtained for GAPDH protein, using ImageJ image processing program (National Institutes of Health, Bethesda, MD, http://rsb.info.nih.gov/ij).

2.8. Determination of NQO1 enzymatic activity

Twenty-four hours after incubating the cells with treatments in six-well cell culture plates, the cells were washed with PBS, and then 0.5 ml of homogenization buffer (50 mM potassium phosphate, pH 7.4 and 1.15% KCl) was added to each well. The plates were then stored for 24 h in a −80 °C freezer. Thereafter, thawed cells were extracted and homogenized using a Kontes homogenizer at 4 °C before they were centrifuged at 12,000*g* for 20 min, and the supernatant was transferred to new microcentrifuge tubes for determination of protein concentration using the Lowry method (Lowry et al., 1951). NQO1 activity was determined by the continuous spectrophotometric assay of Ernster (Ernster, 1967), which quantitates the reduction of 2,6-dichlorophenolindophenol (DCPIP) by 0.02 mg of cell homogenate protein in the presence of β-nicotinamide adenine dinucleotide phosphate (NADPH; 200 μM) and flavin adenine dinucleotide (FAD; 5 μM). The rate of reduction of DCPIP (40 μM) in 1 ml of Tris–HCl buffer (pH 7.8, 25 mM) containing 0.1% (v/v) Tween 20 and 0.023% bovine serum albumin was monitored for 90 s at 600 nm with $\varepsilon = 2.1\ mM^{-1}\ cm^{-1}$. The NQO1 activity was calculated as the decrease in absorbance per min per mg of total protein of the sample which quantitates the dicoumarol-inhibitable reduction of DCPIP.

2.9. Preparation of nuclear extracts

Nuclear extracts from HepG2 cells were prepared according to a previously described procedure (Andrews et al., 1983) with slight modifications. Briefly, HepG2 cells grown on 100-mm petri dishes were treated for 2 h with vehicle, 1 nM TCDD, or 5 μM SUL in the presence and absence of 100 μM V^{5+}. Thereafter, cells were washed twice with cold PBS, pelleted and suspended in cold buffer A [10 mM Hepes-KOH, 1.5 mm $MgCl_2$, 10 mM KC1, 0.5 mM dithiothreitol and 0.5 mM phenylmethylsulphonyl fluoride (PMSF)] pH 7.9, at 4 °C. After 15 min on ice, the cells were centrifuged at 6500*g* and the pellets were suspended again in high salt concentration cold buffer C (20 mM Hepes-KOH, pH 7.9, 25% glycerol, 420 mM NaCl, 1.5 mM $MgCl_2$, 0.2 mM EDTA, 0.5 mM dithiothreitol and 0.5 mM PMSF) to extract nuclear proteins. The cells were then incubated on ice with vigorous agitation every 5 min for 30 min followed by centrifugation for 10 min at 12,000*g* at 4 °C. The nuclear extracts (supernatant) were stored at −80 °C till further use.

2.10. Transient transfection and luciferase assay

HepG2 cells were plated onto twelve-well cell culture plates. ARE-driven luciferase reporter plasmid PGL3-ARE and the renilla luciferase pRL-CMV vector, used for normalization, were co-transfected into HepG2 cells. Each well of cells was transfected with 1.5 μg of PGL3-ARE (generously provided by Dr. Shinya Ito, University of Toronto, Ontario, Canada) and 0.1 μg pRL-CMV using Lipofectamine 2000 reagent according to the manufacturer's instructions (Invitrogen). The luciferase assay was performed according to the manufacturer's instructions (Promega) as described previously (Elbekai and El-Kadi, 2007). In brief, after incubation with test compounds for 24 h, cells were washed with PBS, 100 μl of 1X passive lysis buffer was added into each well with continuous shaking for at least 20 min, and then the content of each well was collected separately in 1.5 ml microcentrifuge tubes. Enzyme activities were determined using a Dual-Luciferase reporter assay system (Promega). Quantification was performed using a TD-20/20 luminometer (Turner BioSystems, Sunnyvale CA).

2.11. NQO1 mRNA stability

The half-life of NQO1 mRNA was determined by an Act-D chase assay. Cells were pretreated with 1 nM TCDD for 6 h. Thereafter, cells were then washed three times and incubated with 5 μg/ml Act-D to inhibit further RNA synthesis, immediately before treatment with 100 μM V^{5+}. Total RNA was extracted at 0, 6, 12 and 24 h after incubation with V^{5+}. Real-time PCR reactions were performed using SYBR Green PCR Master Mix. The fold change in the level of NQO1 (target gene) between treated and untreated cells, corrected by the level of β-actin, was determined using the following equation: Fold change = $2^{-\Delta(\Delta Ct)}$, where $\Delta Ct = Ct_{(target)} - Ct_{(ß\text{-actin})}$ and $\Delta(\Delta Ct) = \Delta Ct_{(treated)} - \Delta Ct_{(untreated)}$.

2.12. NQO1 protein stability

The half-life of NQO1 protein was analyzed by the CHX chase assay. Cells were pretreated with 1 nM TCDD for 24 h. Thereafter, cells were then washed three times and incubated with 10 μg/ml CHX, to inhibit further protein synthesis, immediately before treatment with 100 μM V^{5+}. Cell homogenates were extracted at 0, 6, 12, 24, 36 and 48 h after incubation with V^{5+}. Cellular protein was determined using the method of Lowry (Lowry et al., 1951). NQO1 protein was measured by Western blotting. The intensity of NQO1 protein bands was quantified, relative to the signals obtained for GAPDH protein, using ImageJ software. The protein

half-life values were determined from semilog plots of integrated densities versus time.

2.13. Statistical analysis

The comparative analysis of the results from various experimental groups with their corresponding controls was performed using SigmaStat for Windows (Systat Software, Inc., San Jose, CA). A one-way analysis of variance followed by the Student-Newman-Keul test was carried out to assess statistical significance. For dose-dependency significance, *t* test between different V^{5+} treatments was performed. The differences were considered significant when $P < 0.05$.

3. Results

3.1. Concentration-dependent effect of V^{5+} on TCDD-mediated induction of NQO1 mRNA

To examine the ability of V^{5+} to modulate NQO1 gene expression, HepG2 cells were treated with various concentrations of V^{5+} in the presence of 1 nM TCDD. Thereafter, NQO1 mRNA was assessed using real-time PCR. The concentrations of V^{5+} used hereafter were chosen after determining the ability of wide range of concentrations to modulate the NQO1 gene expression without significantly affecting cell viability (Abdelhamid et al., 2010). Initially, TCDD alone caused 228% increase in NQO1 mRNA levels that was inhibited in a dose-dependent manner by V^{5+}, starting at the lowest concentration tested which is 25 μM (20%), and reaching the maximum inhibition at the concentration of 250 μM (70%) (Fig. 1A).

3.2. Concentration-dependent effect of V^{5+} on TCDD-mediated induction of NQO1 protein and catalytic activity

To examine whether the observed inhibitory effect of V^{5+} on the NQO1 mRNA is reflected at the protein and catalytic activity levels, HepG2 cells were treated for 24 h with increasing concentrations of V^{5+} in the presence of 1 nM TCDD. Our results show that TCDD alone caused 382% and 173% increase in NQO1 protein and catalytic activity levels, respectively. On the other hand, V^{5+} significantly reduced the TCDD-mediated induction of NQO1 at the protein and activity levels in a dose-dependent manner (Fig. 1B and C). V^{5+} at the concentration of 25 μM inhibited the TCDD-mediated induction of NQO1 protein expression level by 33%. At the catalytic activity level, the inhibition started at 50 μM where V^{5+} inhibited the TCDD-mediated induction of NQO1 protein level by 16%. On the other hand, the maximal inhibition took place with the highest concentration tested, 250 μM V^{5+}, in which the TCDD-mediated induction of NQO1 protein and catalytic activity levels were inhibited by 80% and 37% in comparison to the TCDD-induced NQO1 protein and catalytic activity levels (Fig. 1B and C).

3.3. Concentration-dependent effect of V^{5+} on SUL-mediated induction of NQO1 mRNA, protein and catalytic activity

The fact that V^{5+} inhibited TCDD-mediated induction of NQO1 gene expression raised the question whether V^{5+} will behave similarly in the presence of SUL which induces NQO1 gene expression through the Nrf2 pathway only. For this purpose, HepG2 cells were treated with 5 μM SUL in the presence and absence of V^{5+}. If V^{5+} exerts its effect solely through the AhR pathway; we expect to see limited effect of V^{5+} on the SUL-mediated induction of NQO1. Our results shows that SUL alone significantly increased NQO1 mRNA levels by 214% that was inhibited in a dose-dependent manner by V^{5+}, starting at the lowest concentration tested 25 μM (32%), and reaching the maximum inhibition at the concentration of 250 μM (69%) (Fig. 2A). Furthermore, this inhibition was further translated to the protein and catalytic activity levels, in which SUL alone showed a significant induction of NQO1 protein and catalytic activity levels by 329% and 195%, respectively (Fig. 2B and C). On the other hand, V^{5+} significantly reduced the SUL-mediated induction of NQO1 at the protein and activity levels in a dose-dependent manner (Fig. 2B and C). The inhibition started at V^{5+}

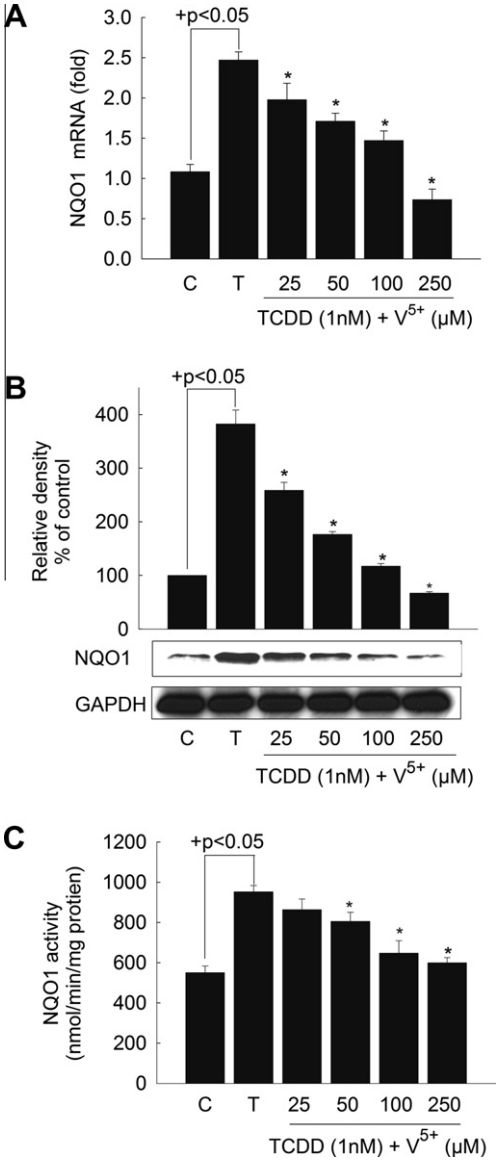

Fig. 1. Concentration-dependent effect of V^{5+} on TCDD-mediated induction of NQO1 at mRNA, protein and catalytic activity in HepG2 cells. HepG2 cells were treated with increasing concentrations of V^{5+} in the presence of 1 nM TCDD for 6 h for mRNA or 24 h for protein and catalytic activity. (A) First-strand cDNA was synthesized from total RNA (1.5 μg) extracted from HepG2 cells. cDNA fragments were amplified and quantitated using ABI 7500 real-time PCR system as described under Section 2. Duplicate reactions were performed for each experiment, and the values presented are the means of three independent experiments. (+) $P < 0.05$, compared to control (C) (concentration = 0 μM); (∗) $P < 0.05$, compared to respective TCDD (T) treatment. (B) Protein (5 μg) was separated on a 10% SDS–PAGE. NQO1 protein was detected using the enhanced chemiluminescence method. The intensity of bands was normalized to GAPDH signals, which was used as loading control. One of three representative experiments is shown. (C) NQO1 enzyme activity was determined spectrophotometrically using DCPIP as substrate. Values are presented as mean ± SE ($n = 6$). (+) $P < 0.05$, compared to control (C); (∗) $P < 0.05$, compared to respective TCDD (T) treatment.

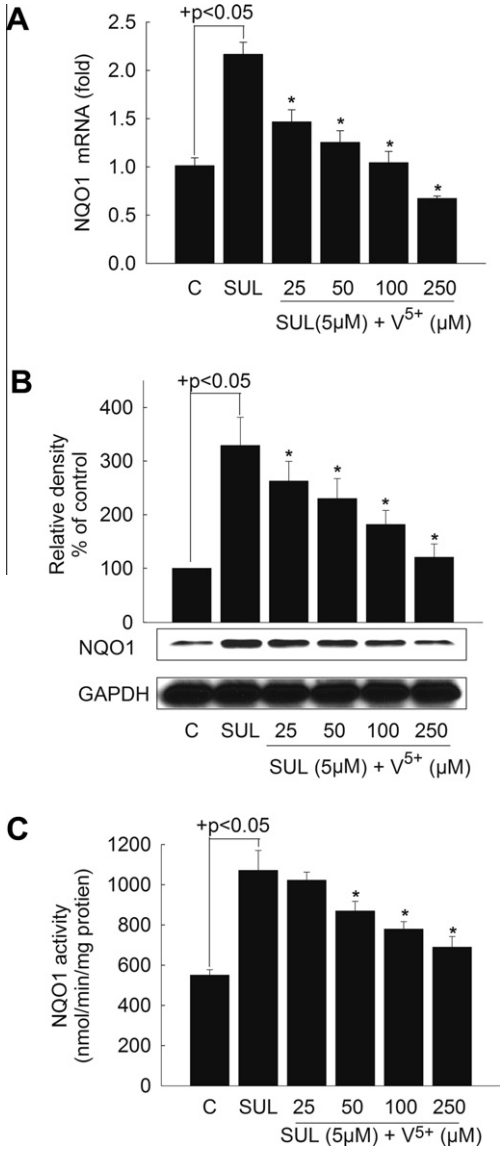

Fig. 2. Concentration-dependent effect of V^{5+} on SUL-mediated induction of NQO1 at mRNA, protein and catalytic activity in HepG2 cells. HepG2 cells were treated with increasing concentrations of V^{5+} in the presence of 5 μM SUL for 6 h for mRNA or 24 h for protein and catalytic activity. (A) First-strand cDNA was synthesized from total RNA (1.5 μg) extracted from HepG2 cells. cDNA fragments were amplified and quantitated using ABI 7500 real-time PCR system as described under Section 2. Duplicate reactions were performed for each experiment, and the values presented are the means of three independent experiments. (+) $P < 0.05$, compared to control (C) (concentration = 0 μM); (∗) $P < 0.05$, compared to respective SUL treatment. (B) Protein (5 μg) was separated on a 10% SDS–PAGE. NQO1 protein was detected using the enhanced chemiluminescence method. The intensity of bands was normalized to GAPDH signals, which was used as loading control. One of three representative experiments is shown. (C) NQO1 enzyme activity was determined spectrophotometrically using DCPIP as substrate. Values are presented as mean ± SE ($n = 6$). (+) $P < 0.05$, compared to control (C); (∗) $P < 0.05$, compared to respective SUL treatment.

concentrations of 25 and 50 μM by 20% and 30%, respectively at the protein level, and by 5% and 19%, respectively at the catalytic activity level, and reached the maximum inhibition at the concentration of 250 μM by 64% and 36% with NQO1 protein and catalytic activity, respectively (Fig. 2B and C).

3.4. Transcriptional inhibition of NQO1 gene by V^{5+}

To determine if the observed effect upon co-exposure to V^{5+} and TCDD on NQO1 is occurring through an ARE-dependent mechanism, HepG2 cells were transiently transfected with the ARE-driven luciferase reporter gene. Luciferase activity results showed that 100 μM V^{5+} alone did not alter the luciferase activity. TCDD (1 nM) and SUL (5 μM) were capable of causing a significant induction of the luciferase activity by 215% and 181%, respectively, as compared with control. On the other hand, co-treatment with V^{5+} (100 μM) decreased the luciferase activity by 26% and 23% compared to TCDD and SUL alone, respectively (Fig. 3).

3.5. Effect of V^{5+} on the levels of Nrf2

In the current study we showed that V^{5+} decreased TCDD- and SUL-mediated induction of NQO1 mRNA at the transcriptional level. Therefore, it was of interest to examine the effect of V^{5+} on the Nrf2 mRNA levels. Our results demonstrated that V^{5+} did not affect the gene expression of Nrf2 (Fig. 4A). Thus, V^{5+} mediated inhibition of NQO1 gene expression is not occurring through the inhibition of Nrf2 transcription.

In an attempt to investigate whether V^{5+} inhibited Nrf2 accumulation via increasing its degradation we measured the Nrf2 protein levels in the total cell lysate of HepG2 cells treated with V^{5+} for different time points. Our results demonstrated that V^{5+} did not affect the short-lived Nrf2 protein at all time points tested (Fig. 4B). Thus V^{5+}-mediated inhibition of either TCDD or SUL-mediated induction of NQO1 is not occurring through increasing Nrf2 protein degradation.

In an effort to determine whether V^{5+} interferes with the nuclear translocation of Nrf2 to the ARE, we examined the potential effect of V^{5+} on TCDD- and SUL-induced translocation of Nrf2 to the nucleus using Western blot analysis. For this purpose, HepG2 cells were treated with vehicle, V^{5+}, TCDD, TCDD plus V^{5+}, SUL and SUL plus V^{5+}, for 2 h, followed by extraction of nuclear extracts. Our results showed that V^{5+} alone did not affect the nuclear accumulation of Nrf2. On the other hand, TCDD and SUL increased the nuclear accumulation of Nrf2 (Fig. 4C). Interestingly, we found that V^{5+} was able to inhibit the TCDD- and SUL-induced nuclear accumulation of Nrf2, suggesting that V^{5+} inhibits the nuclear accumulation through either decreasing the Nrf2 protein level or inhibiting its nuclear translocation.

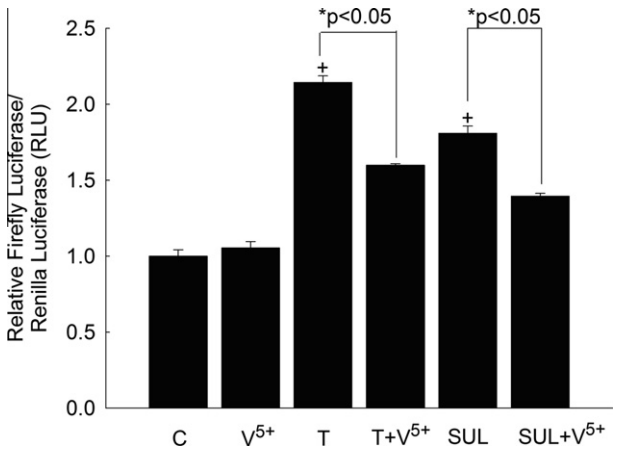

Fig. 3. Effect of V^{5+} on ARE-dependent luciferase activity. HepG2 cells were transiently co-transfected with the reporter plasmid PGL3-ARE and the renilla luciferase pRL-CMV vector. Cells were treated with vehicle, V^{5+} (100 μM), TCDD (1 nM), TCDD (1 nM) + V^{5+} (100 μM), SUL (5 μM) or SUL (5 μM) + V^{5+} (100 μM) for 24 h. Thereafter, cells were lysed, and luciferase activity was measured according to the manufacturer's instruction. Luciferase activity is reported as relative light units (RLU). Values are presented as mean ± SE ($n = 3$). (+) $P < 0.05$, compared with control (C); (∗) $P < 0.05$, compared with the respective TCDD (T) or SUL treatment.

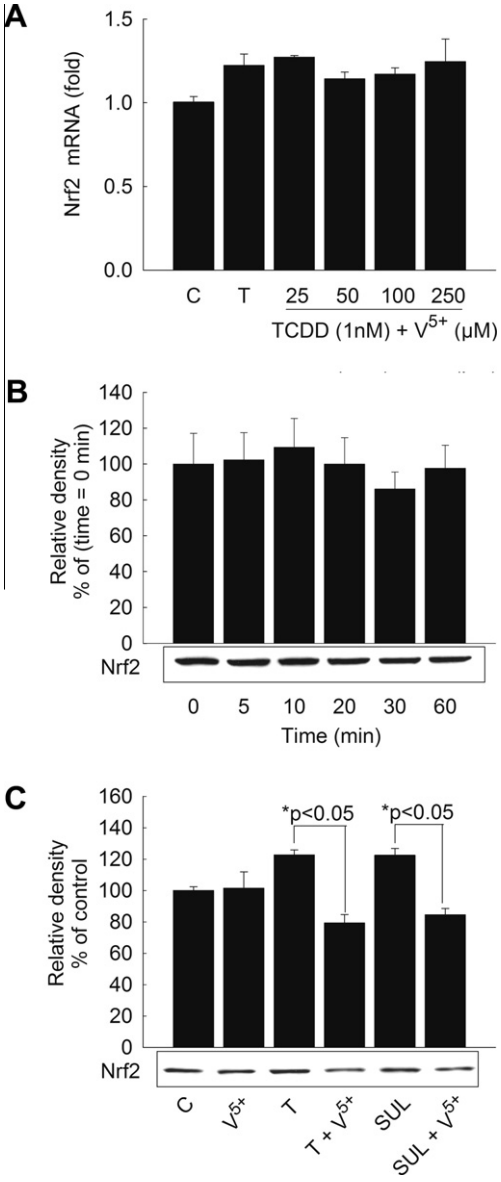

Fig. 4. Effect of V^{5+} on Nrf2 mRNA (A), total Nrf2 protein level (B) and nuclear accumulation of Nrf2 protein (C). (A) HepG2 cells were treated with increasing concentrations of V^{5+} in the presence of 1 nM TCDD for 6 h. First-strand cDNA was synthesized from total RNA (1.5 μg) extracted from HepG2 cells. cDNA fragments were amplified and quantitated using ABI 7500 real-time PCR system as described under Section 2. Duplicate reactions were performed for each experiment, and the values presented are the means of three independent experiments. (B) HepG2 cells treated with V^{5+} for different time points. Total cell lysate protein (25 μg) was separated on a 10% SDS–PAGE. Nrf2 protein was detected using the enhanced chemiluminescence method. The intensity of bands was normalized to GAPDH signals (not shown), which was used as loading control. One of three representative experiments is shown. (+) $P < 0.05$, compared to control (C); (∗) $P < 0.05$, compared to respective TCDD (T) or SUL treatment. (C) HepG2 cells were treated for 2 h with vehicle, V^{5+} (100 μM), TCDD (1 nM), TCDD (1 nM) + V^{5+} (100 μM), SUL (5 μM) or SUL (5 μM) + V^{5+} (100 μM). Thereafter, nuclear proteins (25 μg) were separated on a 10% SDS–PAGE. Nrf2 protein was detected using the enhanced chemiluminescence method. One of three representative experiments is shown.

3.6. Post-transcriptional modification of NQO1 mRNA by V^{5+}

The level of mRNA expression is a function of the transcription rate, and the elimination rate, through processing or degradation. Therefore, we examined the effect of V^{5+} on the stability of human NQO1 mRNA transcripts, using an Act-D chase experiment. Our results showed that NQO1 mRNA is a long-lived mRNA with a half-life of 27.76 ± 5.85 h (Fig. 5). On the other hand, co-exposure to V^{5+} and TCDD did not significantly alter the NQO1 mRNA level compared with TCDD alone, indicating that the decrease in NQO1 mRNA transcripts in response to V^{5+} was not due to any increase in its degradation.

3.7. Post-translational modification of NQO1 protein by V^{5+}

It was of interest to examine the effect of V^{5+} on the turnover rate of the final gene product, the NQO1 protein. In an attempt to examine the involvement of post-translational mechanisms in the modulation of NQO1 activity by V^{5+}, the effect of V^{5+} on NQO1 protein half-life was determined using CHX chase experiment. Fig. 6 shows that NQO1 protein induced by TCDD degraded with a half-life of 44.62 ± 2.04 h. Interestingly, V^{5+} significantly decreased the stability of NQO1 protein which degraded with a half-life of 33.56 ± 2.85 h (Fig. 6).

4. Discussion

Research on the possible biological and metabolic roles of V^{5+} in organisms has increased over the last three decades. In the early

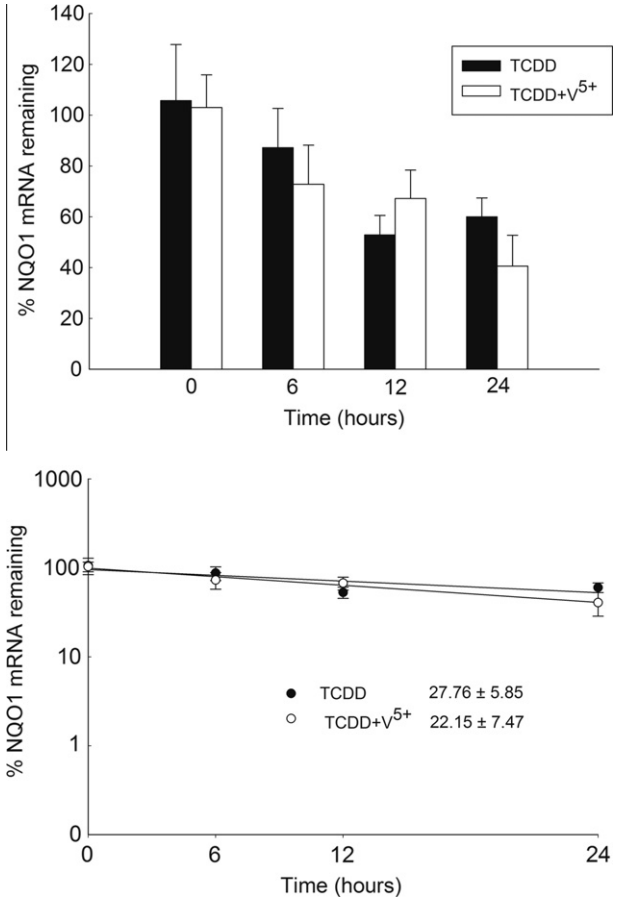

Fig. 5. Effect of V^{5+} on NQO1 mRNA half-life. HepG2 cells were grown to 90% confluence in six-well cell culture plates and were treated with 1 nM TCDD for 6 h. The cells were then washed three times and incubated in fresh media containing 100 μM V^{5+} plus 5 μg/ml Act-D, a RNA synthesis inhibitor. First-strand cDNA was synthesized from total RNA (1.5 μg) extracted from HepG2 cells. cDNA fragments were amplified and quantitated using an ABI 7500 real-time PCR system as described under Section 2. mRNA decay curves were analyzed individually, and the half-life was estimated from the slope of a straight line fitted by linear regression analysis to a semilog plot of mRNA amount, expressed as a percentage of treatment at time = 0 h (maximum, 100%) level, versus time. The half-lives obtained from three independent experiments were then used to calculate the mean half-life (mean ± S.E., $n = 3$).

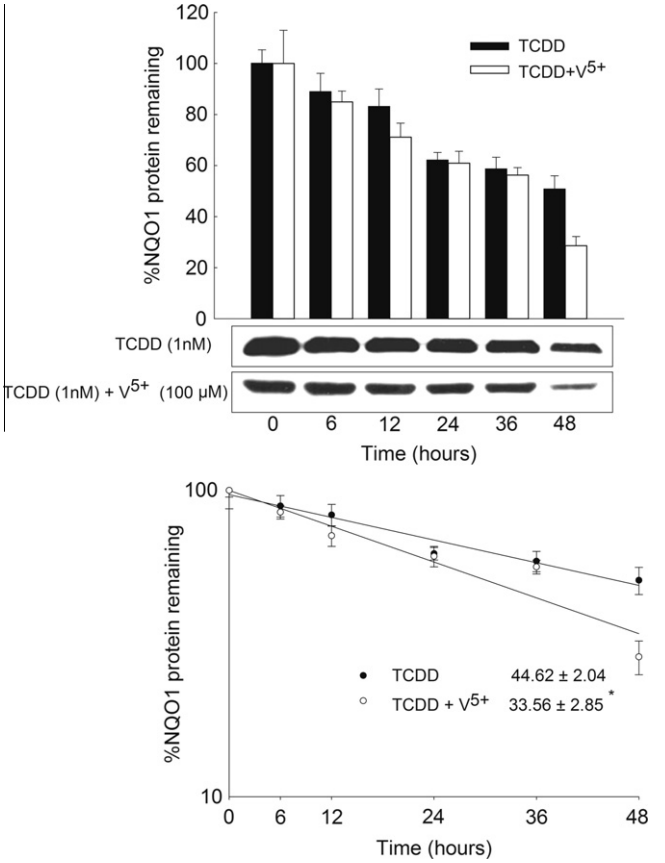

Fig. 6. Effect of V^{5+} on the NQO1 protein half-life. HepG2 cells were grown to 90% confluence in six-well cell culture plates. Thereafter, the cells were treated with 1 nM TCDD for 24 h. Cells were washed and incubated in fresh media containing 100 μM V^{5+} plus 10 μg/ml CHX, a protein translation inhibitor. Protein was extracted at the designated time points after the addition of CHX. Protein (5 μg) was separated by 10% SDS–PAGE and transferred to a nitrocellulose membrane. The intensities of NQO1 protein bands were normalized to GAPDH signals, which were used as loading controls. All protein decay curves were analyzed individually. The half-life was estimated from the slope of a straight line fitted by linear regression analysis to a semilog plot of protein amount, expressed as a percentage of treatment at time = 0 h (maximum, 100%) level, versus time. The half-lives obtained from three independent experiments were then used to calculate the mean half-life (mean ± S.E., $n = 3$). (*) $P < 0.05$ compared with TCDD.

seventies, vanadium was reported to be an essential trace element for chicken and rats (Pham Huu and Chanvattey, 1967) and this has lead to predicate if vanadium could also be essential for human (Sabbioni et al., 1996). There are two important aspects related to vanadium as a trace element. Firstly, its essentiality for mammalian growth (Barrio and Etcheverry, 2006), and the demonstrated biological effects which it produces, including depression of cholesterol and triglyceride metabolism, influence the shape of erythrocytes, and stimulate glucose oxidation and glycogen synthesis in the liver (Dickerson and Charland, 2002). Secondly, its release in large quantities to the atmosphere from the combustion of fossil fuels (Dundar, 2006; Sabbioni et al., 1996).

Recent data suggest that V^{5+} compounds exert protective effects against chemical-induced carcinogenesis, mainly through modifying various xenobiotic metabolizing enzymes (Evangelou, 2002). Yet, it has been seen that high V^{5+} concentrations are found in tissue samples of actual tumors as compared to those in normal tissues (Evangelou, 2002). Interestingly, we have shown previously that V^{5+} down-regulates the NQO1 gene expression in murine Hepa 1c1c7 through a transcriptional mechanism, possibly through inhibiting the ATP-dependent activation of Nrf2. Data from our laboratory and others showed that heavy metals other than V^{5+} are capable of modifying NQO1 through different stages of its regulatory pathway. Therefore, the objectives of the current study were to examine the effect of V^{5+} on the expression of human NQO1 using human hepatoma HepG2 cells, and to investigate the underlying mechanisms involved in this modulation.

In the current study we hypothesize that V^{5+} down-regulates the inducible NQO1 gene expression through inhibiting both the AhR and Nrf2 signaling pathways. Hence the main objective of the current study was to determine the potential effect of co-exposure to V^{5+} and TCDD or SUL, as bifunctional and monofunctional inducers, respectively, on NQO1 gene expression. Our results clearly demonstrated that V^{5+} significantly inhibited the TCDD- and SUL-mediated induction of NQO1 at mRNA, protein and activity levels in HepG2 cells. These results suggest that V^{5+} inhibits NQO1 expression through the AhR/XRE and the Nrf2/ARE signaling pathways.

Being able to inhibit inducible NQO1 gene expression in addition to its similar previous reported effect on CYP1A1 (Abdelhamid et al., 2010), V^{5+} was suspected to exert its effect through inhibiting the transcription of Nrf2. To address this question we examined the effect of V^{5+} on the Nrf2 mRNA level. Our results demonstrated that V^{5+} did not affect the mRNA levels of Nrf2, further confirming that the inhibitory effect of V^{5+} on NQO1 gene expression was not due to any decrease in the expression of Nrf2.

The transcriptional regulation of NQO1 gene expression by V^{5+} was supported by a series of evidence, the first being its ability to inhibit TCDD- and SUL-mediated induction of NQO1 mRNA in a dose-dependant manner. Secondly, V^{5+} was able to inhibit the TCDD- and SUL-induced ARE-luciferase activity. Thirdly, V^{5+} was able to inhibit the TCDD- and SUL-induced nuclear accumulation of Nrf2. Finally, V^{5+} was not able to significantly alter the NQO1 mRNA half-life.

Inhibition of adenosinetriphosphatase (ATPase) by V^{5+} was extensively studied (Cantley et al., 1977, 1978; North and Post, 1984). Since one of the two NQO1 regulatory pathways involves activation and subsequent translocation of the AhR, it is thus expected that V^{5+} through inhibiting the ATP-dependent translocation of AhR would inhibit the NQO1 gene expression. In addition, it has been previously reported that the Nrf2 activity is ATPase-dependent (Zhang et al., 2006). Bearing in mind that V^{5+} is a potent ATPase inhibitor, it is not surprising to observe a decrease in Nrf2 nuclear accumulation in response to V^{5+}. Therefore, our results suggest that the inhibitory effect of V^{5+} on the NQO1 gene expression is occurring primarily through an ATP-dependent mechanism.

Despite the fact that V^{5+} inhibited the nuclear accumulation of Nrf2 protein, there was still a possibility that V^{5+} might have participated in increasing the degradation of Nrf2 protein through its well known 26S proteasomal pathway. Therefore, we examined the time-dependent effect of V^{5+} on the total Nrf2 protein levels. Our results demonstrated that V^{5+} did not affect the total Nrf2 protein levels, further confirming that V^{5+} inhibited the Nrf2 translocation to the nucleus without affecting its protein levels.

We have previously shown that heavy metals do not affect the NQO1 mRNA and protein turn-over rates (Korashy and El-Kadi, 2006). Yet it was of great importance to determine the effect of V^{5+} on the NQO1 mRNA and protein half-life. The cellular mRNA level at any time point is a function of the rate of its production, through transcriptional mechanism, and the rate of its degradation. Our results showed that NQO1 transcripts are long-lived with an estimated half-lives of approximately 27.8 ± 5.9 h; V^{5+} was unable to decrease the NQO1 mRNA half-life. Furthermore, our results showed that NQO1 is a long-lived protein with an estimated half-life of 44.6 ± 2.0 h, interestingly; our results showed that V^{5+} significantly decreased the NQO1 protein half-life by 25% compared to TCDD alone. In contrary to our results, we have previously shown in Hepa 1c1c7 cells that V^{5+} increase NQO1 protein stability

(Anwar-Mohamed and El-Kadi, 2008). These results suggest that the effect of V^{5+} on NQO1 protein stability is species-specific.

In conclusion, the present study demonstrates that V^{5+} down-regulates human NQO1 gene expression primarily through a transcriptional mechanism. Furthermore, Nrf2 nuclear accumulation is inhibited by V^{5+}. This is the first study to report the effect V^{5+} on human detoxifying enzyme NQO1, and may provide further evidence for V^{5+}-induced carcinogenesis.

Acknowledgments

This work was supported by Natural Sciences and Engineering Research Council of Canada (NSERC) Discovery Grant RGPIN 250139-07 to A.O.S. G.A. is the recipient of Egyptian government Scholarship award. A.A.-M. is the recipient of Alberta Ingenuity Graduate Scholarship award. We are grateful to Dr. Shinya Ito (University of Toronto, Ontario, Canada) for providing us with the human ARE luciferase reporter plasmid PGL3-ARE.

References

Abdelhamid, G., Anwar-Mohamed, A., Badary, O.A., Moustafa, A.A., El-Kadi, A.O., 2010. Transcriptional and posttranscriptional regulation of CYP1A1 by vanadium in human hepatoma HepG2 cells. Cell Biol. Toxicol.

Ai, D., Pang, W., Li, N., Xu, M., Jones, P.D., Yang, J., Zhang, Y., Chiamvimonvat, N., Shyy, J.Y., Hammock, B.D., Zhu, Y., 2009. Soluble epoxide hydrolase plays an essential role in angiotensin II-induced cardiac hypertrophy. Proc Natl Acad Sci USA 106, 564–569.

Andrews, P., Thomas, H., Pohlke, R., Seubert, J., 1983. Praziquantel. Med. Res. Rev. 3, 147–200.

Anwar-Mohamed, A., El-Kadi, A.O., 2008. Down-regulation of the carcinogen-metabolizing enzyme cytochrome P450 1a1 by vanadium. Drug Metab. Dispos. 36, 1819–1827.

Anwar-Mohamed, A., El-Kadi, A.O., 2009. Down-regulation of the detoxifying enzyme NAD(P)H:quinone oxidoreductase 1 by vanadium in Hepa 1c1c7 cells. Toxicol. Appl. Pharmacol. 236, 261–269.

Baran, E.J., 2008. Vanadium detoxification: chemical and biochemical aspects. Chem. Biodivers. 5, 1475–1484.

Barceloux, D.G., 1999. Vanadium. J. Toxicol. Clin. Toxicol. 37, 265–278.

Barrio, D.A., Etcheverry, S.B., 2006. Vanadium and bone development: putative signaling pathways. Can. J. Physiol. Pharmacol. 84, 677–686.

Cantley Jr., L.C., Josephson, L., Warner, R., Yanagisawa, M., Lechene, C., Guidotti, G., 1977. Vanadate is a potent (Na, K)-ATPase inhibitor found in ATP derived from muscle. J. Biol. Chem. 252, 7421–7423.

Cantley Jr., L.C., Resh, M.D., Guidotti, G., 1978. Vanadate inhibits the red cell (Na^+, K^+) ATPase from the cytoplasmic side. Nature 272, 552–554.

Chen, X.L., Kunsch, C., 2004. Induction of cytoprotective genes through Nrf2/antioxidant response element pathway: a new therapeutic approach for the treatment of inflammatory diseases. Curr. Pharm. Des. 10, 879–891.

Dickerson, R.N., Charland, S.L., 2002. The effect of sepsis during parenteral nutrition on hepatic microsomal function in rats. Pharmacotherapy 22, 1084–1090.

Dundar, M.S., 2006. Vanadium concentrations in settled outdoor dust particles. Environ. Monit. Assess. 123, 345–350.

Edel, J., Sabbioni, E., 1989. Vanadium transport across placenta and milk of rats to the fetus and newborn. Biol. Trace Elem. Res. 22, 265–275.

Elbekai, R.H., El-Kadi, A.O., 2007. Transcriptional activation and posttranscriptional modification of Cyp1a1 by arsenite, cadmium, and chromium. Toxicol. Lett. 172, 106–119.

Ernster, L., 1967. DT diaphorase. Methods Enzymol. 10, 309–317.

Evangelou, A.M., 2002. Vanadium in cancer treatment. Crit. Rev. Oncol. Hematol. 42, 249–265.

Haiman, C.A., Hankinson, S.E., De Vivo, I., Guillemette, C., Ishibe, N., Hunter, D.J., Byrne, C., 2003. Polymorphisms in steroid hormone pathway genes and mammographic density. Breast Cancer Res. Treat. 77, 27–36.

Hankinson, O., 1995. The aryl hydrocarbon receptor complex. Annu. Rev. Pharmacol. Toxicol. 35, 307–340.

Iida, K., Itoh, K., Kumagai, Y., Oyasu, R., Hattori, K., Kawai, K., Shimazui, T., Akaza, H., Yamamoto, M., 2004. Nrf2 is essential for the chemopreventive efficacy of oltipraz against urinary bladder carcinogenesis. Cancer Res. 64, 6424–6431.

Itoh, K., Chiba, T., Takahashi, S., Ishii, T., Igarashi, K., Katoh, Y., Oyake, T., Hayashi, N., Satoh, K., Hatayama, I., Yamamoto, M., Nabeshima, Y., 1997. An Nrf2/small Maf heterodimer mediates the induction of phase II detoxifying enzyme genes through antioxidant response elements. Biochem. Biophys. Res. Commun. 236, 313–322.

Korashy, H.M., El-Kadi, A.O., 2006. Transcriptional regulation of the NAD(P)H:quinone oxidoreductase 1 and glutathione S-transferase ya genes by mercury, lead, and copper. Drug Metab. Dispos. 34, 152–165.

Lee, J.M., Johnson, J.A., 2004. An important role of Nrf2-ARE pathway in the cellular defense mechanism. J. Biochem. Mol. Biol. 37, 139–143.

Lee, J.S., Surh, Y.J., 2005. Nrf2 as a novel molecular target for chemoprevention. Cancer Lett. 224, 171–184.

Livak, K.J., Schmittgen, T.D., 2001. Analysis of relative gene expression data using real-time quantitative PCR and the $2^{-\Delta\Delta CT}$ method. Methods 25, 402–408.

Lowry, O.H., Rosebrough, N.J., Farr, A.L., Randall, R.J., 1951. Protein measurement with the Folin phenol reagent. J. Biol. Chem. 193, 265–275.

Ma, Q., Kinneer, K., Bi, Y., Chan, J.Y., Kan, Y.W., 2004. Induction of murine NAD(P)H:quinone oxidoreductase by 2,3,7,8-tetrachlorodibenzo-p-dioxin requires the CNC (cap 'n' collar) basic leucine zipper transcription factor Nrf2 (nuclear factor erythroid 2-related factor 2): cross-interaction between AhR (aryl hydrocarbon receptor) and Nrf2 signal transduction. Biochem. J. 377, 205–213.

Meyer, B.K., Pray-Grant, M.G., Vanden Heuvel, J.P., Perdew, G.H., 1998. Hepatitis B virus X-associated protein 2 is a subunit of the unliganded aryl hydrocarbon receptor core complex and exhibits transcriptional enhancer activity. Mol. Cell Biol. 18, 978–988.

Miao, W., Hu, L., Scrivens, P.J., Batist, G., 2005. Transcriptional regulation of NF-E2 p45-related factor (NRF2) expression by the aryl hydrocarbon receptor-xenobiotic response element signaling pathway: direct cross-talk between phase I and II drug-metabolizing enzymes. J. Biol. Chem. 280, 20340–20348.

Motohashi, H., Yamamoto, M., 2004. Nrf2-Keap1 defines a physiologically important stress response mechanism. Trends Mol. Med. 10, 549–557.

Nechay, B.R., 1984. Mechanisms of action of vanadium. Annu. Rev. Pharmacol. Toxicol. 24, 501–524.

Nioi, P., Hayes, J.D., 2004. Contribution of NAD(P)H:quinone oxidoreductase 1 to protection against carcinogenesis, and regulation of its gene by the Nrf2 basic-region leucine zipper and the arylhydrocarbon receptor basic helix-loop-helix transcription factors. Mutat. Res. 555, 149–171.

North, P., Post, R.L., 1984. Inhibition of (Na, K)-ATPase by tetravalent vanadium. J. Biol. Chem. 259, 4971–4978.

Pham Huu, C., Chanvattey, S., 1967. Comparative study of sodium chromate, molybdate, tungstate and metavandate. V. Experiments on pigeons, chickens and rats. Agressologie 8, 433–439.

Prochaska, H.J., Santamaria, A.B., 1988. Direct measurement of NAD(P)H:quinone reductase from cells cultured in microtiter wells: a screening assay for anticarcinogenic enzyme inducers. Anal. Biochem. 169, 328–336.

Prochaska, H.J., Talalay, P., 1988. Regulatory mechanisms of monofunctional and bifunctional anticarcinogenic enzyme inducers in murine liver. Cancer Res. 48, 4776–4782.

Rushmore, T.H., Kong, A.N., 2002. Pharmacogenomics, regulation and signaling pathways of phase I and II drug metabolizing enzymes. Curr. Drug Metab. 3, 481–490.

Rushworth, S.A., MacEwan, D.J., O'Connell, M.A., 2008. Lipopolysaccharide-induced expression of NAD(P)H:quinone oxidoreductase 1 and heme oxygenase-1 protects against excessive inflammatory responses in human monocytes. J. Immunol. 181, 6730–6737.

Sabbioni, E., Kueera, J., Pietra, R., Vesterberg, O., 1996. A critical review on normal concentrations of vanadium in human blood, serum, and urine. Sci. Total Environ. 188, 49–58.

Sambrook, J., Fritsch, E.F., Maniatatis, T., 1989. Molecular Cloning. Cold Spring Harbour Laboratory Press, New York.

Westerink, W.M., Schoonen, W.G., 2007. Phase II enzyme levels in HepG2 cells and cryopreserved primary human hepatocytes and their induction in HepG2 cells. Toxicol. In Vitro 21, 1592–1602.

Whitelaw, M.L., Gustafsson, J.A., Poellinger, L., 1994. Identification of transactivation and repression functions of the dioxin receptor and its basic helix-loop-helix/PAS partner factor Arnt: inducible versus constitutive modes of regulation. Mol. Cell Biol. 14, 8343–8355.

Xu, C., Li, C.Y., Kong, A.N., 2005. Induction of phase I, II and III drug metabolism/transport by xenobiotics. Arch. Pharm. Res. 28, 249–268.

Yu, X., Kensler, T., 2005. Nrf2 as a target for cancer chemoprevention. Mutat. Res. 591, 93–102.

Zhang, J., Ohta, T., Maruyama, A., Hosoya, T., Nishikawa, K., Maher, J.M., Shibahara, S., Itoh, K., Yamamoto, M., 2006. BRG1 interacts with Nrf2 to selectively mediate HO-1 induction in response to oxidative stress. Mol. Cell Biol. 26, 7942–7952.